Proceedings of the 2007 American Control Conference
Marriott Marquis Hotel at Times Square
New York City, USA, July 11-13, 2007

Wave-Based Time Delay Compensation in Bilateral Teleoperation: Two-Channel versus Four-Channel Architectures

A. Aziminejad, M. Tavakoli, R.V. Patel, M. Moallem

Department of Electrical and Computer Engineering, University of Western Ontario, London, ON N6A 5B9, Canada
Canadian Surgical Technologies & Advanced Robotics (CSTAR), 339 Windermere Road, London, ON N6A 5A5, Canada

***Abstract*— In this paper, two different approaches have been proposed aiming to improve transparency of a passivity-based delay-compensated teleoperation system: direct force reflection in a two-channel wave-based control architecture, which uses the same number of channels as the traditional position error-based control scheme with wave variables and, four-channel wave-based control architecture, which is capable of achieving ideal transparency in the presence of time delay. In order to present a comprehensive performance comparison, we quantify the transparency of each approach through subjecting the experimental results of a bilateral master-slave system developed for endoscopic surgery applications to identification of the hybrid parameters of the equivalent two-port network.**

I. Introduction

A bilateral teleoperation system provides a means for bidirectional transmission of data between a master and a remote slave unit with a time delay between them. The main goals of teleoperation are stability and transparency. It has been demonstrated that the four-channel (4CH) architecture is the best teleoperation architecture from a transparency point of view with no time delays [1], [2], [3]. In the presence of time delays, the stability and transparency of a bilateral teleoperation system are severely affected. An extensive review and comparison concerning various time delay compensation methods is given in [4].

Scattering approaches which inherently preserve passivity are theoretically able to stabilize a teleoperation system independent of transmission delays [5]. A more physically motivated reformulation of these ideas led to the introduction of wave theory [6], which provides a framework for designing and analyzing bilateral teleoperation systems. However, so far these concepts have only been applied to a two-channel (2CH) position error-based (PEB) teleoperation system. In this paper, we will utilize the wave transformation technique in a 2CH teleoperation architecture which is based upon kinesthetic feedback of direct force measurements at the slave side. Using experimental results, we show that this control scheme can improve transparency without imposing additional cost on stability of the teleoperation system. Keeping in mind the unrivalled advantage of the 4CH architecture from a transparency perspective for the delay-free condition, we extend wave theory in a manner which can be applied to the 4CH architecture, and compare the transparency of an optimized 4CH architecture and its less complex three-channel (3CH) derivative with that of a 2CH architecture in terms of the hybrid parameters of the equivalent two-port network. All our conclusions are validated by experimental results.

This research was supported by the Natural Sciences and Engineering Research Council (NSERC) of Canada under grants RGPIN-1345 and RGPIN-227612, the Ontario Research and Development Challenge Fund under grant 00-May-0709 and infrastructure grants from the Canada Foundation for Innovation awarded to the London Health Sciences Centre (CSTAR) and the University of Western Ontario.

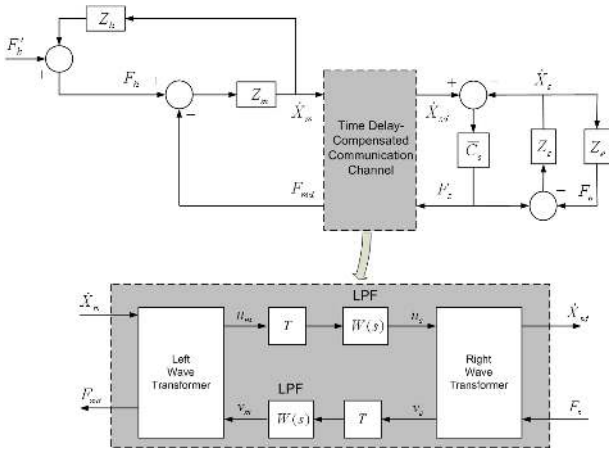

Fig. 1. Wave-based delay compensated PEB 2CH teleoperator.

II. Wave Theory Framework

We assume the following single DOF equations of motions for the master and the slave manipulators throughout our work:

$$M_m\ddot{x}_m = -f_m + f_h \qquad M_s\ddot{x}_s = f_s - f_e \tag{1}$$

where M_m and M_s are the master and slave inertias, f_m and f_s are the master and slave control actions, and x_m and x_s are the master and slave positions. Also, f_h and f_e represent the interaction forces between the operator's hand and the master, and the slave and the remote environment, respectively. By considering velocities and forces in a teleoperation system as currents and voltages, an equivalent electrical circuit representation of the system can be obtained. This equivalent circuit representation can be expressed by the following hybrid model:

$$\begin{bmatrix} F_h \\ -\dot{X}_s \end{bmatrix} = \begin{bmatrix} h_{11} & h_{12} \\ h_{21} & h_{22} \end{bmatrix} \cdot \begin{bmatrix} \dot{X}_m \\ F_e \end{bmatrix}$$

To achieve ideally transparent bilateral teleoperation system in the presence of time delay, the concept of transparency in [1], [3] can be further extended to the delayed kinematic correspondence and the delayed interaction force correspondence ($V_s = e^{-sT}V_m$ and $F_h = e^{-sT}F_e$, respectively). Consequently, the hybrid matrix of a delayed ideally transparent teleoperation system takes the following form:

$$H = \begin{bmatrix} 0 & e^{-sT} \\ -e^{-sT} & 0 \end{bmatrix} \tag{2}$$

The wave variable approach for time delay compensation in bilateral teleoperation stems from scattering theory and theoretically guarantees stability under arbitrary time delay as long as the incoming and outgoing wave signals experience a fixed amount of time delay. The original position error-based wave transformation method proposed in [6] for a 2CH

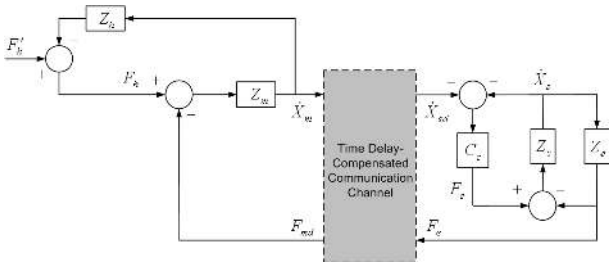

Fig. 2. 2CH wave-based direct force reflection teleoperator.

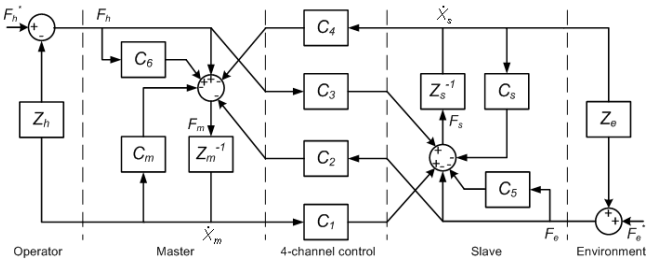

Fig. 3. 4CH bilateral teleoperation system without time delay.

teleoperation architecture encodes power variables velocity and force $(\dot{x}, f)$ pre-transmission, as wave variables u and v, as shown in Figure 1. The corresponding transformation at the master side is defined as

$$u_m = (b\dot{x}_m + f_{md})/\sqrt{2b} \quad v_m = (b\dot{x}_m - f_{md})/\sqrt{2b} \qquad (3)$$

where b denotes the characteristic wave impedance, which is a positive constant. In this system, $Z_m = M_m s$ and $Z_s = M_s s$ represent impedances of the single-DOF master and slave robots, respectively and and F_h' is the exogenous input force from the operator. The PD controller $\bar{C}_s(s)$ is used for position control at the slave side. Upon arrival at the slave side, velocity and force information are extracted from the received wave variables. The slave side post-reception transformation is

$$u_s = (b\dot{X}_{sd} + F_s)/\sqrt{2b} \quad v_s = (b\dot{X}_{sd} - F_s)/\sqrt{2b} \qquad (4)$$

Theoretically speaking, systems expressed in wave variables become completely robust to delays of any amount or phase lags of any level. In practice, a wave-based teleoperation system performance can be degraded due to a number of reasons, among which are discrete implementation of continuous-time control laws and significant variations in the operator's behavior or the environment impedance. The performance is particularly degraded for large time delays where high frequency oscillations appear in the teleoperation system. The idea of filtering the wave variables was initially suggested in [6] for noise reduction and frequency shaping, especially when the proposed impedance matching scheme fails to achieve the goal of transparency improvement [7]. In this research, we use lowpass filters $W(s)$ in the wave domain as shown in Figure 1.

III. 2CH Architectures

Depending on the choice of input/output pairs from the four variables in equations (3) and (4), we distinguish four different wave transformation arrangements. These four passivity-based time delay compensation architectures are position-force (i.e. position control at the master side and force control at the slave side), force-position, position-position, and force-force. Both Anderson and Spong [5] and Niemeyer and Slotine [6] have avoided the use of force sensor measurements in bilateral teleoperation control because of their inherent noisy nature and questions that may arise about the passivity of the whole system. Including force sensor measurements in time-delay teleoperation control has been shown to improve transparency while stability can still be maintained [8].

Figure 2 depicts a 2CH wave-based direct force teleoperation reflection architecture, in which measurements of hand-master and slave-environment interaction forces are used. In this system we assume the PD position controller at the slave side has the form $\bar{C}_s(s) = (k_d s + k_p)/s$. It is worth mentioning that the 2CH PEB and direct force reflection architectures of Figure 1 and Figure 2 possesses a non-symmetric scattering matrix. Therefore, an analytic absolute stability study based on scattering matrix analysis tends to become mathematically untractable for both of them [8]. Moreover, in the case of the direct force reflection architecture, the scattering matrix is not reciprocal either implying that, although sufficient, passivity is not a necessary condition for its stability. The interest in passivity of a teleoperation system stems from the fact that it ensures robustly stable performance for a class of multivariable systems that cannot be easily subjected to other methods of stability analysis, usually at the cost of performance. In practice, it was observed that by utilizing two additional lowpass filters in the system, one for filtering the measured slave/environment interaction force f_e before feeding it to the slave-side wave transformer and the other for filtering the reflected force f_{md} before applying it to the master robot, it is possible to have better loop-shaping flexibility in order to obtain the best stable performance in the teleoperation system. It can be shown that even in the absence of any force sensor noise, these low-pass filters help to improve transparency by pushing the maximum singular values of the scattering matrix of the direct force reflection teleoperation system towards unity. The precise tuning of these filters depends on the characteristic of the force sensor and is basically an implementation issue.

IV. 4CH Architecture

A. Delay-free case

Figure 3 depicts a general 4CH bilateral teleoperation architecture [1], [2]. The operator and environment exogenous forces F_h' and F_e' are inputs independent of teleoperation system behavior. This architecture can represent all teleoperation structures through appropriate selection of subsystem dynamics C_1 to C_6. In contrast to 2CH architectures, a sufficient number of parameters (degrees of freedom) in the 4CH architecture enables it to achieve ideal transparency. The local force feedback compensators C_5 and C_6 improve stability and performance of the system [3]. Perfect transparency is achieved if and only if the hybrid matrix in (2) has the following form

$$H = \begin{bmatrix} 0 & 1 \\ -1 & 0 \end{bmatrix} \qquad (5)$$

which has been obtained from (2) by taking $T = 0$. Applying the perfect transparency conditions (5) to the hybrid parameters of Figure 3, the following ideal transparency condition

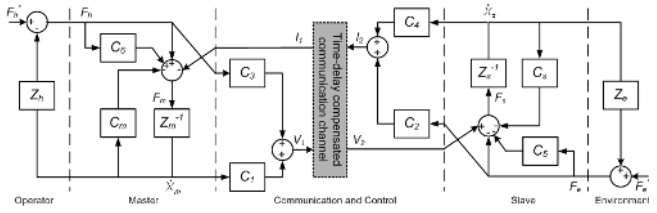

Fig. 4. Wave-based 4CH teleoperation system.

set is derived for the 4CH architecture:

$$C_1 = Z_{ts} \quad C_2 = 1 + C_6 \quad C_3 = 1 + C_5 \quad C_4 = -Z_{tm} \quad (6)$$

where $Z_{tm} = M_m s + C_m(s) = M_m s + k_{dm} + k_{pm}/s$ and $Z_{ts} = M_s s + C_s(s) = M_s s + k_{ds} + k_{ps}/s$, assuming C_m and C_s to be PD controllers.

B. Wave-Based 4CH Architecture

So far the passivity-based time delay compensation approach has been applied only to 2CH architectures. In order to extend this approach to a 4CH teleoperation architecture, we need to segregate the communication channel part of the system in Figure 3 as a two-port network. Figure 4 shows a possible method for accomplishing this extension. The non-physical input effort and flow pair for this two-port network model of the communication channel are

$$V_1 = C_3 F_h + C_1 \dot{X}_m \qquad I_2 = C_2 F_e + C_4 \dot{X}_s \quad (7)$$

The master and the slave closed-loop equations can be written as $\dot{X}_m Z_m = -\dot{X}_m C_m + F_h(1 + C_6) - I_1$ and $\dot{X}_s Z_s = -\dot{X}_s C_s - F_e(1 + C_5) + V_2$. Therefore, the non-physical output flow and effort pair are

$$I_1 = F_h(1 + C_6) - \dot{X}_m Z_{tm} \quad V_2 = F_e(1 + C_5) + \dot{X}_s Z_{ts} \quad (8)$$

The communication channel effort and flow relationships in (7) and (8), from which the input and output pseudo-power functions are calculated, are not unique but in their presented form they are independent of knowledge of Z_e and Z_h, which is an advantage for implementation. Moreover, it can be easily checked that for the case of $T = 0$, $V_1 = V_2$ and $I_1 = I_2$, thus the original system of Figure 3 is recovered. The communication channel can be modelled based on its inputs and outputs as

$$\begin{bmatrix} -I_1 \\ V_2 \end{bmatrix} = \begin{bmatrix} c_{11} & c_{12} \\ c_{21} & c_{22} \end{bmatrix} \begin{bmatrix} V_1 \\ I_2 \end{bmatrix} = C(s) \begin{bmatrix} V_1 \\ I_2 \end{bmatrix} \quad (9)$$

where the matrix C can be defined with respect to the hybrid matrix of the communication channel as

$$C(s) = H_{ch}^{-1}(s) \quad (10)$$

The outputs of the wave transformation block at the master side are

$$I_1 = (\sqrt{2b}u_m - V_1)/b \quad v_m = (bu_m - \sqrt{2b}V_1)/b \quad (11)$$

and at the slave side are

$$V_2 = bI_2 - \sqrt{2b}v_s \quad u_s = \sqrt{2b}I_2 - v_s \quad (12)$$

Transformation (11) can be derived from the basic definition of wave variables (i.e., equation (3)) by taking the flow variable (I_1) and v_m as the outputs and the effort variable (V_1) and u_m as the inputs. Similarly, wave transformation (12) is obtained from (4) through selecting V_2 and u_s as the outputs and I_2 and v_s as the inputs. This arrangement results from the fact that the input/output relationship for the communication channel of the proposed 4CH architecture corresponds to an "inverse hybrid" representation of a two-port network (i.e., its inputs are V_1 and I_2 and its outputs are $-I_1$ and V_2, where the directions of the input and output flows correspond to the convention set in [5]) – see equation (10), whereas that relationship is in the form of a hybrid model for the 2CH architecture of Figure 1.

C. Transparency considerations and 3CH architecture

Applying condition set (6) for ideal transparency without time delay, the overall hybrid parameters of the proposed wave-based 4CH teleoperation system in Figure 4 are given by:

$$\begin{aligned} h_{11} &= [(W^2 e^{-2sT} - 1)(Z_{ts}^2 - b^2 Z_{tm}^2)]/D_2 \\ h_{12} &= 2bWe^{-sT}(Z_{tm}C_3 + Z_{ts}C_2)/D_2 \\ h_{21} &= -2bWe^{-sT}(Z_{tm}C_3 + Z_{ts}C_2)/D_2 \\ h_{22} &= [(W^2 e^{-2sT} - 1)(b^2 C_2^2 - C_3^2)]/D_2 \end{aligned} \quad (13)$$

where

$$\begin{aligned} D_2 &= b(W^2 e^{-2sT} + 1)(Z_{ts}C_2 + Z_{tm}C_3) \\ &+ (W^2 e^{-2sT} - 1)(-b^2 C_2 Z_{tm} - C_3 Z_{ts}) \end{aligned} \quad (14)$$

For asymptotic convergence of the position and torque errors in Figure 3, the controller gains should be chosen in accordance with [9] as:

$$C_s/C_m = M_s/M_m \quad (15)$$

Using (15), it can be easily shown that $Z_{ts}/Z_{tm} = M_s/M_m$. Setting h_{11} from (13) equal to zero under the ideal transparency condition according to (2) gives:

$$b_{\text{ideal}} = Z_{ts}/Z_{tm} \quad (16)$$

Similarly, for h_{22} to be equal to zero, we should have

$$C_3/C_2 = b_{\text{ideal}} \quad (17)$$

Using (16) and (17) in (13), expressions for h_{12} and h_{21} under ideal transparency condition can be derived as:

$$h_{12} = -h_{21} = W(s)e^{-sT} \quad (18)$$

Equation (18) means that for $W(s) = 1$, the condition set (6) along with equations (16) and (17) are delayed ideal transparency provisions for the proposed 4CH architecture of Figure 4. It can be shown that a teleoperation system represented by the delayed ideally transparent hybrid matrix in (2) cannot preserve passivity [5]. Therefore, a stability study in this case also needs to factor Z_h and Z_e. For the teleoperation system under ideal transparency conditions, if Z_{ts} is Hurwitz ($k_{ds}, k_{ps} > 0$), the input admittance transfer function based on the input F_h' and the output $\dot{X}_m$ can be simplified to

$$Y_{\text{in}} = (Z_h + Z_e e^{-2sT})^{-1} \quad (19)$$

In order to present a descriptive stability analysis of an ideally transparent delayed teleoperation system, it is possible to use Pade approximation to simplify the characteristic polynomial in (19) and apply the Routh-Hurwitz theorem assuming $Z_h = (M_h s^2 + k_{dh} s + k_{ph})/s$ and $Z_e = k_{pe}/s$. For mathematical tractability, we use a first-order Pade

approximation $e^{-2sT} \simeq (1 - sT)/(1 + sT)$ to re-write the characteristic equation in (19) as

$$M_h T s^3 + (k_{dh} T + M_h) s^2 + (-k_{ph} \alpha T + k_{ph} T + k_{dh}) s + k_{ph} \alpha + k_{ph} = 0 \quad (20)$$

where $\alpha = k_{pe}/k_{pm}$. Applying Routh-Hurwitz theorem to (20), the following condition on α as the necessary and sufficient condition for stability of the system represented by (19) will be derived

$$\alpha = \frac{k_{pe}}{k_{ph}} < \frac{k_{dh}(M_h + k_{dh} T + k_{ph} T^2)}{k_{ph}(2M_h + k_{dh} T) T} \quad (21)$$

Equation (21) sets an upper bound on the remote environment stiffness k_{pe} depending on the operator parameters and time delay. Generally speaking, condition (21) is easy to meet particularly under small delays or with compliant environments, or through operator's adaptation to the remote environment characteristics.

Another potential benefit of the general 4CH architecture of Figure 3 is that by proper adjustment of the local feedback parameters, it is possible to obtain two classes of 3CH control architectures, which can be transparent under ideal conditions [3], [9]. The first class of 3CH architectures is derived by setting $C_2 = 1$ and $C_3 = 0$. As a consequence, $C_5 = -1$ and $C_6 = 0$. In other words, there is no need for any master/operator interaction force measurements and therefore, the number of the sensors in the system can be reduced. The second class of 3CH architectures is obtained by setting $C_2 = 0$ and $C_3 = 1$. In this class, force measurements at the slave side are not needed. The use of fewer sensors without incurring any penalty on system transparency makes the 3CH architectures extremely attractive from the implementation point of view.

Deriving a wave-based 3CH architecture from the proposed wave-based 4CH architecture under ideal transparency provisions only affects h_{22}. In order to explain this further, assume under condition set (6) and provisions (15) and (16) that only the slave unity local force feedback is used (i.e., $C_5 = -1$ and $C_6 = 0$). It can be easily shown that h_{11}, h_{12}, and h_{21} still keep their ideal transparency values after this rearrangement. However, the new h_{22} is

$$h_{22} = (W^2 e^{-2sT} - 1)/(2Z_{tm}) \quad (22)$$

According to (22), the bigger the magnitude of Z_{tm}, the closer h_{22} is to its ideal value of zero. This result suggests that this 3CH architecture is suitable for applications in which the master is heavy. On the other hand, if only the master unity local force feedback is used (i.e., $C_6 = -1$ and $C_5 = 0$), while h_{11}, h_{12}, and h_{21} remain unchanged from their ideal transparency values, the new h_{22} is given by

$$h_{22} = (1 - W^2 e^{-2sT})/(2Z_{ts}) \quad (23)$$

which shows that the second 3CH architecture is suitable for applications with a heavy slave robot.

V. Experimental Performance Evaluation

For experimental performance evaluation, we have used a force-reflective master-slave system developed as an endoscopic surgery test-bed (Figure 5). Through the master interface, a user controls the motion of the slave surgical tool and receives force/torque feedback of the slave-environment interactions. For details about this master-slave system, the reader is referred to [10]. In the experiments in this paper, the master and slave subsystems were constrained for force-reflective teleoperation in the twist direction only (i.e. rotations about the instrument axis). The user twists the master back and forth causing the slave to repeatedly probe a soft tissue (foam) phantom using a small rigid beam attached to the slave's end-effector (Figure 5) for about 60 seconds. The instrument interactions with the tissue are measured and reflected in real-time to the user. In the haptic interface, the friction/gravity effects are determined and compensated for such that the user does not feel any weight on his/her hand when the slave is not in contact with an object. The digital control loop is implemented at a sampling frequency of 1000 Hz. The master and the slave effective inertias have been identified to be $M_m = 5.968 \times 10^{-4}$ kgm^2 and $M_s = 9.814 \times 10^{-3}$ kgm^2, respectively.

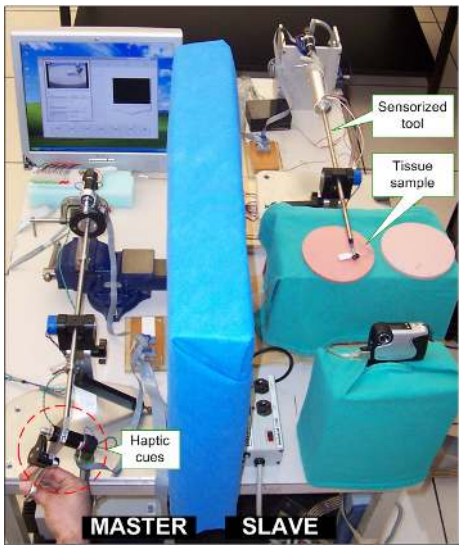

Fig. 5. Master-slave experimental setup.

Figure 6 shows the master and the slave position and torque tracking profiles for a PEB teleoperation architecture with $b = 1$, $T = 100$ ms, $k_d = 3$, $k_p = 10$, and $f_{\text{cut}} = 5$ Hz. Assuming that a dedicated communication network will be used, our choice of one-way time delay of 100 ms is conservative since coast-to-coast round trip communication delays are expected to be of the order of 60 ms. Figure 7 illustrates the same tracking profiles for a modified direct force reflection teleoperation architecture with similar parameters, where the cut-off frequency for f_e and f_{md} first-order filters is 2 Hz. As can be deduced from these figures, the position tracking performance for the two systems are close to each other. However, the modified direct force reflection teleoperation system displays a superior force tracking performance, which demonstrates a higher level of transparency. This deduction is in accordance with the results presented in [11] for teleoperation systems without time delay.

To further investigate the relative transparency of these two systems, a second set of free-motion tests was performed, which in conjunction with the previous contact-mode tests, can be used to determine the hybrid parameters of the teleoperation system in the frequency domain [8]. The magnitudes of the hybrid parameters of the 2CH PEB and direct force reflection teleoperation architectures for $T = 100$ ms are

shown in Figure 8. Due to the human operator's limited input bandwidth, these identified hybrid parameters can be considered valid up to a frequency of 60 rad/s. Figure 8 is an indication of the superiority of the direct force reflection architecture in terms of transparent performance considering the ideal transparency requirements in the presence of a communication channel time delay, as specified by (2). The hybrid parameter $h_{11} = F_h/X_m|_{F_e=0}$ is the input impedance in free-motion condition. High values of h_{11} for position error-based architecture are evidence of the fact that even when the slave is in free space, the user will feel some force as a result of any control inaccuracies (i.e., nonzero position errors), thus giving a "sticky" feel of free-motion movements. On the other hand, since direct force reflection architecture uses f_e measurements, its input impedance in free-motion condition will be significantly lower making the feeling of free space much more realistic. The parameter $h_{12} = F_h/F_e|_{X_m=0}$ is a measure of force tracking for the haptic teleoperation system. The better force tracking performance of direct force reflection architecture in Figure 8, i.e., $h_{12} \approx 0$ dB, confirms the time-domain results observed in Figures 6 and 7. The parameter $h_{21} = -X_s/X_m|_{F_e=0}$ is a measure of the position tracking performance. In this respect, the spectrum of the PEB architecture is a little closer to 0 dB, which is indicative of a slightly better position tracking performance. It is worthwhile mentioning that because of the finite stiffness of the slave and also the backlash present in the slave's gearhead, the accuracy of $h_{22} = -X_s/F_e|_{X_m=0}$ estimates is less than that of the rest of the hybrid parameters. As can be seen in Figure 6, with the the PEB architecture, there are vibrations in the master and slave positions and forces in the contact mode. It was also observed that the magnitudes of these vibrations increase with time delay. While stability in the wave-based time delay compensation approach is guaranteed in theory regardless of the time delay, in practice and consistent with previous studies [5], [6], such vibrations exist and may be due to implementation reasons such as discretization or limited controller bandwidth. As can be seen in Figure 8, these vibrations affect the h_{12} parameter of the PEB teleoperation architecture. However, as shown in the force profile of Figure 7 and the h_{12} spectrum of Figure 8, force tracking is much less subjected to unwanted vibrations in the case of the direct force reflection architecture. These results are indicative of the fact that transparency is improved by providing slave force sensor data to the bilateral control algorithm.

Figure 9 shows the master and the slave positions and torque tracking profiles for a 4CH wave-based architecture based on the ideal transparency criteria (6), (16), and (17) with single-way time delay $T = 100$ ms, $C_2 = C_3 = 0.5$, $b = 8$, $C_m = 40M_m(10 + s)$ (PD position controller), $C_s = 40M_s(10 + s)$, and $f_{cut} = 1$ Hz. Figure 10 shows the same results for an 3CH wave-base architecture with only the unity local force feedback at the slave side (no master local force feedback). All the other parameters are identical. The reason for choosing this type of 3CH architecture is that in our setup, the slave manipulator is sensorized to measure its interaction force with the environment, while in the absence of a force sensor the master uses a system observer for contact force estimation. The results in these two figures indicate that the 3CH architecture is better suited for our setup in comparison with the 4CH architecture. The magnitudes of the hybrid parameters of the wave-based 4CH and 3CH teleoperation architectures are shown in Figure 11. The force and position tracking performances (reflected in the h_{12} and h_{21} spectra of Figure 11) in the case of the 3CH architecture is almost perfect. The superiority of performance in the case of the 3CH architecture can be attributed to the higher gain of the slave local feedback, which allows for a lower level of master force feedforward and consequently, less contribution from the master side force observer. Unlike the case of the 2CH position error based architecture, 4CH and 3CH architectures do not show any sign of vibrations under contact conditions.

In terms of transparency, 3CH architecture can be considered the best among the four teleoperation control architectures under study. Direct force reflection is showing very good transparency, bearing in mind that it only needs the minimum requirement in terms of the communication channel bandwidth. Also, considering the fact that 3CH and 4CH architectures work under ideal transparency conditions (6), (16), and (17), they are more sensitive to system parameter variations in comparison to a more robust controller architecture such as 2CH direct force reflection. With respect to position tracking under contact conditions, which is not reflected in any of the hybrid parameter spectra, it can be concluded from Figures 6, 7, 9, and 10 that the 3CH and 4CH architectures outperform both of the 2CH architectures. This can be attributed to the fact that the 2CH architectures use only one PD controller at the master side, while a 4CH architecture has a second position controller at the master side. The role of this controller becomes more pronounced when F_e is non-zero.

VI. Conclusion

In this paper, we quantitatively compared the performance of two different approaches for wave-based time-delay compensation in a master-slave system. The first approach is based upon the traditional 2CH bilateral wave-based teleoperation control architecture, in which the system is made robust against communication channel latencies through the introduction of wave transformers. We have effectively improved the transparency of this system by making use of direct force sensing data at the slave side without imposing additional costs on the stability of the system. In the second approach, we have extended the use of wave theory for time-delay compensation to a 4CH control architecture. This control architecture is capable of achieving ideal transparency under delay-free conditions and we have shown that this property is maintained in our proposed 4CH wave-based architecture. The experimental performance comparison of the four teleoperation control architectures indicates that while the 3CH wave-based architecture has the best performance, the 2CH direct force reflection control architecture can offer a comparable performance with less implementation complexity and better stability robustness.

References

[1] D. A. Lawrence, "Stability and transparency in bilateral teleoperation," *IEEE Trans. on Robotics and Automation*, vol. 9, no. 5, pp. 624–637, 1993.

[2] Y. Yokokohji and T. Yoshikawa, "Bilateral control of master-slave manipulators for ideal kinesthetic coupling-formulation and experiment," *IEEE Trans. on Robotics and Automation*, vol. 10, no. 5, pp. 605–619, 1994.

[3] K. Hashtrudi-Zaad and S. E. Salcudean, "Transparency in time delay systems and the effect of local force feedback for transparent teleoperation," *IEEE Trans. on Robotics and Automation*, vol. 18, no. 1, pp. 108–114, 2002.

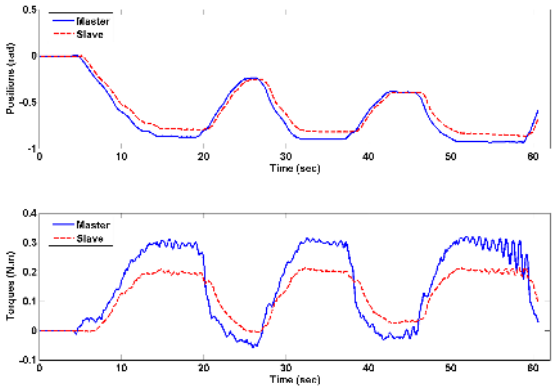

Fig. 6. Position and force tracking profiles for the 2CH PEB teleoperation architecture with one-way delay $T = 100$ ms.

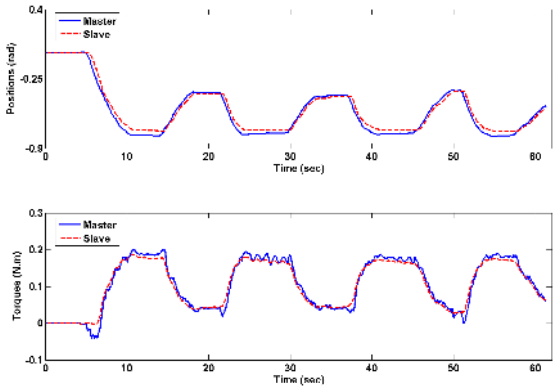

Fig. 9. Position and force tracking profiles for the 4CH wave-based teleoperation architecture with one-way delay $T = 100$ ms.

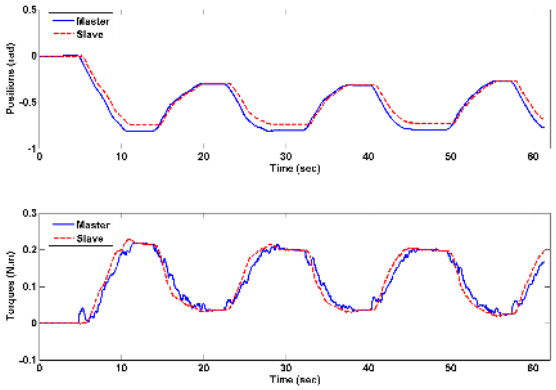

Fig. 7. Position and force tracking profiles for the 2CH direct force reflection (DFR) teleoperation architecture with one-way delay $T = 100$ ms.

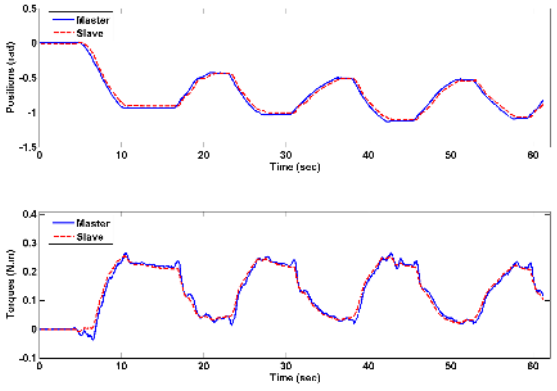

Fig. 10. Position and force tracking profiles for the 3CH wave-based teleoperation architecture with one-way delay $T = 100$ ms.

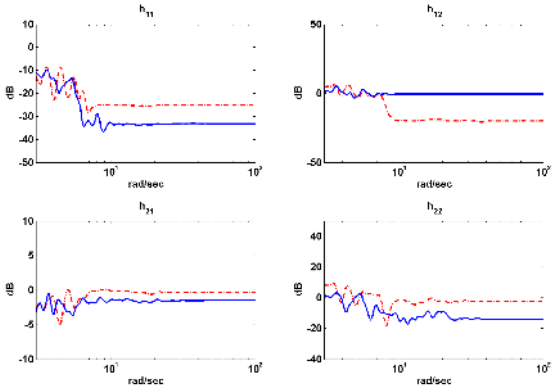

Fig. 8. Magnitudes of the hybrid parameters for the PEB and DFR architectures with one-way delay $T = 100$ ms (dashed: PEB; solid: DFR).

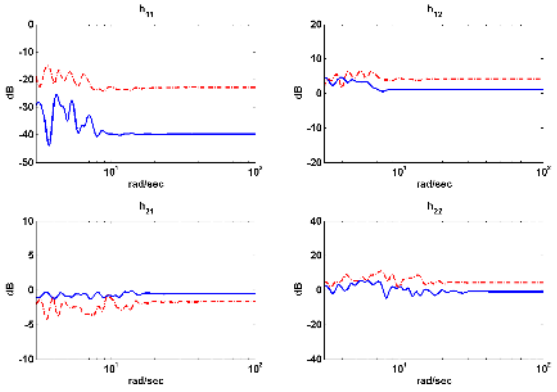

Fig. 11. Magnitudes of the hybrid parameters for the wave-based 4CH and 3CH architectures with one-way delay $T = 100$ ms (dashed: 4CH; solid: 3CH).

[4] P. F. Hokayem and M. W. Spong, "Bilateral teleoperation: An historical survey," *Automatica*, vol. 42, no. 12, pp. 2035–2057, 2006.

[5] R. J. Anderson and M. W. Spong, "Bilateral control of teleoperators with time delay," *IEEE Trans. on Automatic Control*, vol. 34, no. 5, pp. 494–501, 1989.

[6] G. Niemeyer and J. J. E. Slotine, "Stable adaptive teleoperation," *IEEE Journal of Oceanic Eng.*, vol. 16, no. 1, pp. 152–162, 1991.

[7] N. A. Tanner and G. Niemeyer, "High-frequency acceleration feedback in wave variable telerobotics," *IEEE/ASME Trans. on Mechatronics*, vol. 11, no. 2, pp. 119–127, 2006.

[8] A. Aziminejad, M. Tavakoli, R. V. Patel, and M. Moallem, "Bilateral delayed teleoperation: the effects of a passivated channel model and force sensing," *Proc. of IEEE Int. Conf. on Robotics and Automation*, 2007.

[9] M. Tavakoli, R. V. Patel, and M. Moallem, "Bilateral control of a teleoperator for soft tissue palpation: design and experiments," *Proc. of IEEE Int. Conf. on Robotics and Automation*, pp. 3280–3285, 2006.

[10] ——, "A haptic interface for computer-integrated endoscopic surgery and training," *Virtual Reality*, no. 9, pp. 160–176, 2006.

[11] I. Aliaga, A. Rubio, and E. Sanchez, "Experimental quantitative comparison of different control architectures for master-slave teleoperation," *IEEE Trans. on Control Systems Technology*, vol. 12, no. 1, pp. 2–11, 2004.